

SUPPLEMENTAL METHODS

Reagents were obtained from Sigma–Aldrich or Research Products International unless otherwise indicated.

Microscopy in mammalian cells

Cells were induced with 100 ng/ml dox overnight in 12-well poly-D-lysine coated plates (BD). Cells were washed with PBS, and treated with 25 μ M ferric ammonium citrate (FAC), hepcidin (Peptide International) or PR73¹⁵ for 24 hours (concentrations as indicated in figure legends). Cells were visualized with an epifluorescence microscope (Nikon Eclipse), and images were acquired with a 40x objective, SPOT camera, and SPOT Advanced Imaging Software (Diagnostic Instruments).

Fpn membrane localization in mammalian cells

Cells were seeded on 6-well poly-D-lysine coated plates (BD) and induced with 500 ng/ml doxycycline for 24 hours. Cells were washed 3x with PBS and treated with EZ-link maleimide PEG-2-biotin in PBS for 30 minutes at 4 °C. Cells were then washed with 1x PBS, solubilized in RIPA (Boston BioProducts) with protease inhibitors, and Fpn-GFP was immunoprecipitated with anti-GFP Ab as described previously¹⁶. Blots were probed with Streptavidin-HRP (Pierce) and total Fpn was detected with anti-GFP Ab (Roche). To adjust for variations between individual Western blots, we normalized band intensity to WT Fpn sample within the same blot.

Ferritin assay

Cells were processed the same as in the microscopy section. After 24 hours of treatment, cells were washed with PBS and harvested in RIPA with protease inhibitors. Ferritin levels were determined by an ELISA assay (Ramco Laboratories) according to the manufacturer's instructions and were normalized to the total protein concentration in each sample (BCA assay, Pierce). To adjust for variations of the absolute ferritin values between multiple experiments, we expressed the measurements as the relative change in ferritin, according to the formula I/U , where I is the ferritin value for the induced cell line and U is the ferritin value for the uninduced cell line. For hepcidin or PR73-treated cells, we expressed the ferritin measurements as $(H-I)/U$ or $(P-I)/U$, where H refers to the ferritin value for the induced cells treated with hepcidin and P refers to the ferritin value for the induced cells treated with PR73.

Hepcidin binding

Cells were treated with 3 μ g/ml N-terminally biotinylated hepcidin (Peptides International) for 30 min at 37°C. Protein lysates were immunoprecipitated with anti-GFP Ab (Abcam)¹⁶, run under non-reducing conditions, and blotted with Streptavidin-HRP (Pierce). Total Fpn

was blotted with anti-GFP Ab (Roche). To adjust for variations between Western blots, we normalized the values from Fpn mutants to those of WT Fpn within the same blot.

Immunoprecipitation and Western blotting for ubiquitination

Immunoprecipitation was performed as previously¹⁶, except the gel-loading dye contained 5% 2-mercaptoethanol. To adjust for variations between Western blots, we normalized the mutant ubiquitination values to those of the WT within the same blot.

Radioactive iron export for clinical and nonclinical mutants

Adherent cells were loaded with 2 mM ⁵⁵Fe-NTA for 48 hours (prepared from ⁵⁵FeCl₃, Perkin Elmer), washed 3x with medium, re-plated, induced overnight, washed 2x with medium, and then hepcidin was added to some wells. Aliquots of the medium were sampled for up to 10 hours to measure iron export. The “uninduced” measurement at each time point was subtracted as background. The slope of each line was determined and used to calculate the percent iron export by comparing the slopes to that of untreated WT.

Fpn Western blot

Protein was measured by BCA assay, 6x SDS-loading buffer was added to lysates which were then separated by SDS-PAGE on 4-20% Mini-PROTEAN TGX Precast Gels (BioRad), and transferred to PVDF membranes using Trans-Blot Turbo (Bio-Rad). Blocking was performed overnight at 4°C in 5% milk in TBST (50mM Tris-HCl, pH7.5, 150mM NaCl, 0.1% Tween 20). Anti-GFP (Roche) was used to detect Fpn and anti-GAPDH-HRP (Cell Signaling) were used for normalization.

Fpn stability Western blot

Cells were induced with 100 ng/ml doxycycline overnight in 12-well poly-D-lysine coated plates (BD). Next, the medium was removed, cells were washed 2x with 1xPBS, and the zero-time point sample harvested. The remaining wells were treated with 25 μM ferric ammonium citrate (FAC) either with or without 1 μg/ml hepcidin for 24 hours. The protein concentration was measured using the BCA assay and 25 μg of protein per sample was used for Western blots. Anti-GFP Ab (Roche) was used to detect FPN, and normalization was performed using an anti-GAPDH Ab or anti-actin Ab when specified.

Functional expression of hFpn in *Xenopus* oocytes

We performed laparotomy and ovariectomy on adult female *Xenopus laevis* frogs (Nasco) under 2-aminoethylbenzoate methanesulfonate anesthesia (0.2%, by immersion, to effect) following a protocol approved by the University of Cincinnati Institutional Animal Care and Use Committee. The pOX(+) oocyte expression plasmid vectors containing human WT or K8R Fpn-GFP were used to synthesize RNA *in vitro*. We examined the

functional expression of hFpn-GFP and K8R-hFpn-GFP in RNA-injected *Xenopus* oocytes as described¹⁷ except for the following modifications. RNA-injected oocytes were stored at 17 °C in modified Barths' medium (MBM) containing 50 mg.l⁻¹ dox, and incubated 4–5 days before being used in functional assays.

We treated oocytes for 0–4 h with 10 µM hepcidin in MBM prior to assaying iron efflux. Oocytes were injected with 50 nl of 5 µM ⁵⁵Fe, added as Fe³⁺ FeCl₃ (Perkin-Elmer Life Science Products) in a vehicle of composition 250 mM KCl, 5 mM nitrilotriacetic acid trisodium salt, 4 mM 2-(*N*-morpholino)ethanesulfonic acid (GFS Chemicals). To initiate the efflux assay, we placed oocytes in efflux medium of composition 100 mM NaCl, 1 mM KCl, 2 mM CaCl₂, 1 mM MgCl₂, 0.5 mM bathophenanthroline disulfonic acid, 1 mM nitrilotriacetic acid trisodium salt, 50 µg.ml⁻¹ human apotransferrin (R&D Systems), buffered with 2.5 mM 1,4-diethylpiperazine (Alfa Aeser) and approximately 2.5 mM 2-(*N*-morpholino)ethanesulfonic acid to obtain pH 7.5. We obtained the first-order rate constants (*k*) describing iron efflux over 30 min determined for individual oocytes as described¹⁸. Live-cell imaging of Fpn-GFP in oocytes before and after 30-min 10 µM hepcidin treatment was performed as described¹⁷.

Iron export and Fpn Western in human red blood cells

Human packed red blood cells (PRBC, 1 to 10 days old) from four different donors were obtained from the Division of Transfusion Medicine, Department of Pathology and Laboratory Medicine, David Geffen School of Medicine, UCLA, Los Angeles, California. PRBCs were aliquoted and incubated in their storage medium (Anticoagulant Citrate Phosphate Dextrose Adenine Solution, USP, CPDA-1) at 37 °C for 24 h in the presence of 0, 0.4 and 3.6 µM hepcidin or PR73. Samples were collected after 24 h by centrifuging the PRBC at 5,000 g for 8 min. The cell pellet was frozen at -80 °C for further processing. The supernatant was centrifuged again at 5,000 g for 8 min and non-transferrin bound iron (NTBI) measured as previously described¹⁸. Briefly, we used an “enhanced labile plasma iron” (eLPI) assay, based on the catalytic conversion of nonfluorescent dihydrorhodamine to fluorescent rhodamine, in the presence and absence of the iron chelator deferiprone, and a mild metal-mobilizing agent, nitriloacetate.

To measure Fpn protein by Western blotting, cell pellets were lysed in 5 mM sodium phosphate buffer pH 8 with protease and phosphatase inhibitors (Halt protease and phosphatase inhibitors cocktail, Thermo Scientific) to obtain RBC ghost membranes. The membranes were pelleted at 10,000 g for 5 min at 4 °C and washed three times in the same buffer. The resulting pellet was lysed in 80 µl RIPA lysis buffer (Chem Cruz, Santa Cruz) with protease and phosphatase inhibitors, by incubation for 15 min on ice and periodic vortexing. The samples were then centrifuged at 14,000 g for 15 min at 4 °C and the supernatant was used to determine protein concentration using Pierce BCA Protein

Assay Kit (Thermo Scientific) following the manufacturer's protocol. 10 µg protein was loaded on a 4-20% protein gel (Mini Protean TGX gels, BioRad) (samples were not boiled and no reducing agent was added). Proteins were transferred to a Trans Blot Turbo nitrocellulose membrane (BioRad), the membrane was blocked for 1 h with 5% milk dissolved in Tris-buffered saline (Sigma) with 0.1% Tween 20 (TBST, Acros Organics), and incubated with primary antibody (human anti-human ferroportin 38C8, Amgen) overnight at 4 °C at concentration 1 µg/ml, washed and incubated with secondary Goat anti-Human IgG (H+L) Horseradish Peroxidase Conjugate (BioRad) at dilution 1:3000. After washing, the membrane was incubated with Super Signal West Pico chemiluminescent substrate (Thermo Scientific) and imaged using ChemiDoc XRS+ imaging system (BioRad).

Mouse treatment with hepcidin agonists

C57BL/6 mice injected with PR73: Experiments were conducted in accordance with the guidelines by the National Research Council and were approved by the Animal Research Committee of the University of California, Los Angeles. 6-week old male C57BL/6 mice received two intraperitoneal injections 12 hours apart of either solvent SL220 (NOF Corporation) or 60 nmoles PR73 dissolved in SL220, and were analyzed 4 hours after the second injection.

th3 mice injected with minihepcidin M009: th3/+ mice received a single subcutaneous injection of M009¹⁹ (~50 nmoles per mouse), and were analyzed over a time-course of 0-36 h after injection (n=3 per group).

Serum iron was determined as previously described,²⁰ using acid treatment followed by a colorimetric assay for iron quantitation (Sekisui Diagnostics, Charlottetown, Canada). Duodenum Fpn and spleen Fpn were determined by Western blotting as follows: spleen or duodenum was homogenized in lysis buffer, centrifuged, and the supernatant was collected. The protein concentration was determined using the Pierce BCA assay. Samples were run on a 4-15% SDS-PAGE gel without boiling or reducing agent. Once transferred onto nitrocellulose, the blot was blocked in Genscript blocking buffer for 5 minutes. The blot was incubated overnight with rat-anti-mouse Fpn (IC7 from Amgen) in WB-2 buffer from Genscript or monoclonal anti-actin antibody (Sigma) in 5% milk/TTBS overnight at 4 °C. After incubation with secondary antibodies, the blots were imaged using chemiluminescence on ChemiDoc XRS+ imaging system (BioRad). Serum hepcidin was detected using a hepcidin ELISA immunoassay as previously described²¹.

Statistical analysis

We set critical significance level, $\alpha = 0.05$, and expressed our data as mean, SEM for n observations. Statistical analyses employed the two-tailed t-test (normally distributed

data) or Mann-Whitney rank sum test (data with non-normal distribution), the two-tailed one-sample t-test (normally distributed data) or the two-tailed one-sample signed rank test (data with non-normal distribution) compared with a reference of 1, and 2-way analysis of variance (ANOVA). (SigmaPlot version 12.5, Systat Software). The unequal variance t-test was used when the samples failed the equal variance t-test. To account for the possibility of false positives due to multiple comparisons, we determined the significance for each mutant by using the false discovery rate (FDR) correction for multiple comparisons procedure. The significance threshold, α , was set at 0.05. To determine if an individual p-value is significant, the critical level for each comparison is first calculated by α/K_i , where K_i = the rank of the individual comparison (its ranking when compared to other mutants when ordered from highest to lowest p-value). If the individual P value (P_i) is less than the individual critical significance level then that mutant is significantly different from its comparator (designated by * in graphs). The first ranked value of P_i that is greater than its corresponding critical significance level is not significant and all comparisons with a higher P_i are not significant.

Table S1. Primers for site-directed mutagenesis of human Fpn-GFP

Mutation	Forward primer	Reverse primer
S71F	ctggtggtggcagggttgttctggtcctg	caggaccagaacaaaccctgccaccaccag
V72F	ggtggcagggctcttctggtcctggg	cccaggaccagaaaagaccctgccacc
G204S	tggctcccagctcatcagctgtggctttatttc	gaaataaagccacagctgatgactggggagcca
D270V	catctaattgggtgtgaaagtcttaacatccatgagctt	aagctcatggatgttagagactttcacaccattagatg
S338R	cactcagggactgaggggtccatcctcagt	actgaggatggaaccctcagtcctgagtg
Y501C	ggtgtacagaactccatgaactgtcttctgatcttctgc	gcagaagatcaagaagacagttcatggagtctgtacacc
D504N	gtacagaactccatgaactatcttcttaacttctgcatttcatcat	atgatgaaatgcagaagattaagaagatagttcatggagtctgtac
H507R	ctatcttctgatcttctgcgtttcatcatggtcatcctgg	ccaggatgaccatgatgaaacgcagaagatcaagaagatag
F508Y	atcttctgatcttctgcattatcatggtcatcctggctcc	ggagccaggatgaccatgatataatgcagaagatcaagaagat
Y64N	ccaccaccagcccgttactgctgtcaaaag	ctttgacagcagtcaacgggctggtggtgg
N144D	ctattgcaaataattgcagatttgccagtactgc	gcagtactggccaaatctgcaatatttgcaatag
Y333A	accacaggttacgccactcagggactgag	ctcagtcctgagtgccggcgtaccctgtggt
Y333F	cacaggttacgccttactcagggactga	tcagtcctgagtgaggcgtaccctgtg
F324A	tatatgactgtcctgggctgactgcatcaccacagg	cctgtggtgatgcagtcagcggccaggacagtcata
F324Y	tatgactgtcctgggctatgactgcatcaccac	gtggtgatgcagtcatagcccaggacagtcata
C326S	tcctgggcttgacagcatcaccacaggg	ccctgtggtgatgctgtcaaaagcccagga

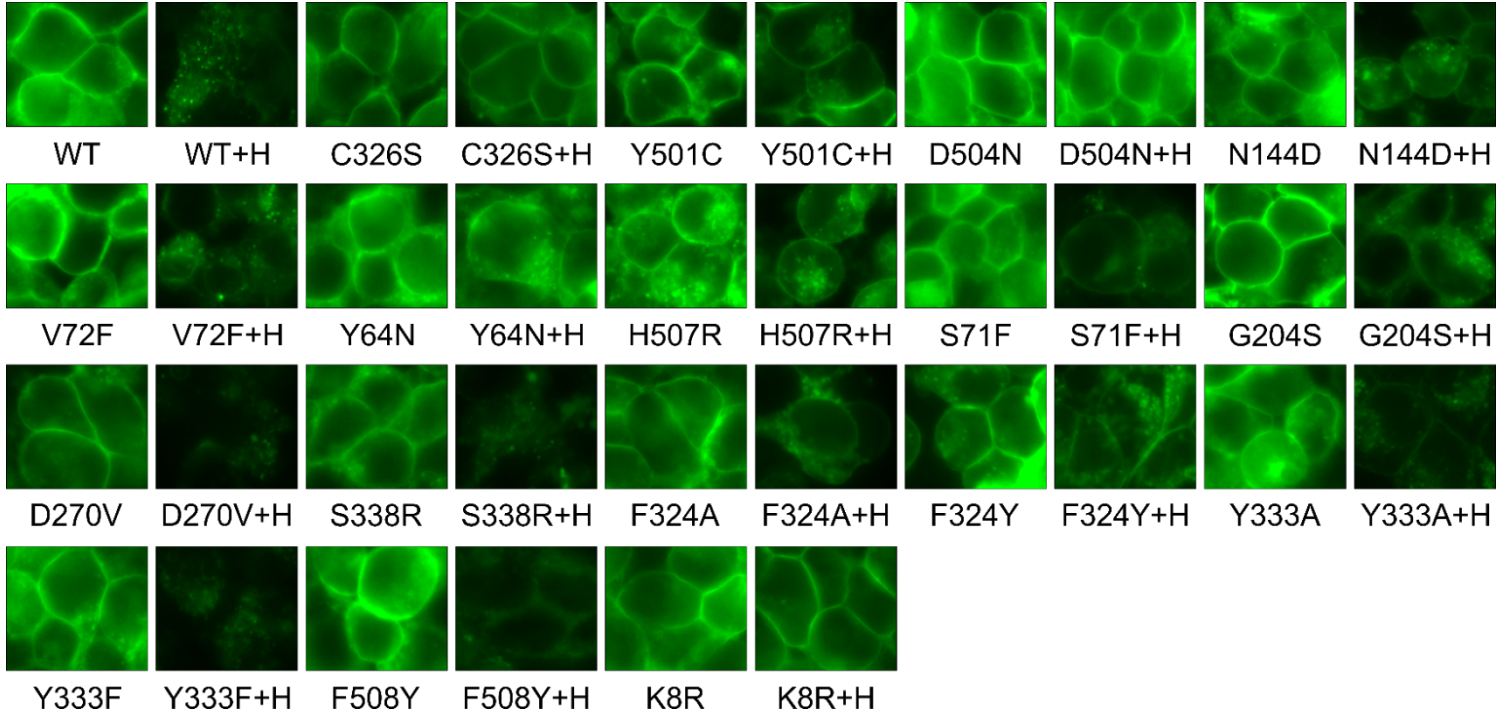


Figure S1: Microscopy of human Fpn (hFpn) mutant cells \pm hepcidin treatment. HEK293T cells stably transfected with doxycycline (dox)-inducible hFpn-GFP mutants were induced with 100 ng/ml dox overnight. The cells were then washed, incubated with $\pm 1 \mu\text{g/ml}$ hepcidin ($0.4 \mu\text{M}$) for 24 hours, and imaged by fluorescent microscopy.

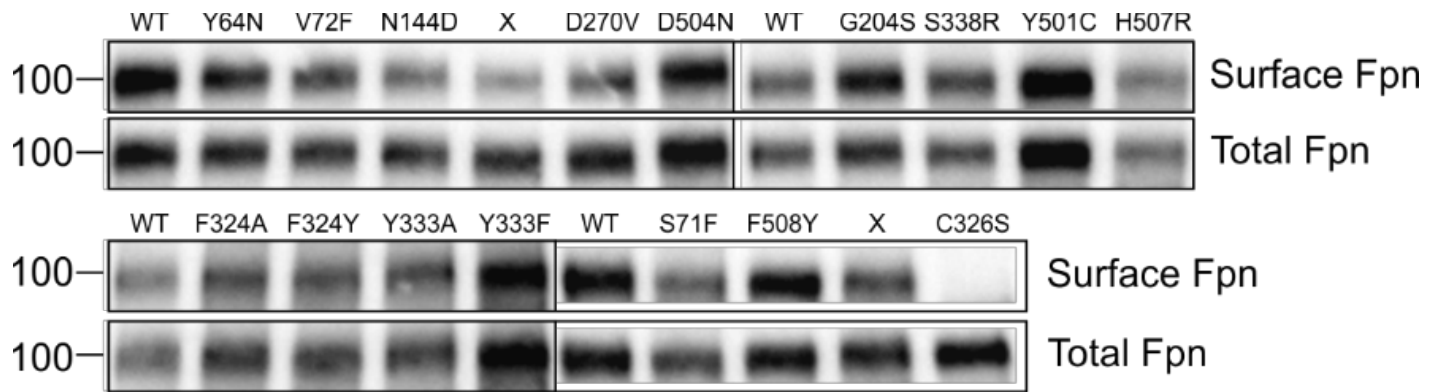


Figure S2: Representative Western blots: cell surface biotinylation of hFpn. HEK293T cells stably expressing doxycycline (dox)-inducible hFpn-GFP mutants were induced with dox to express Fpn, treated with maleimide-biotin for 30 minutes, immunoprecipitated using anti-GFP Ab, and immunoblotted with streptavidin-HRP or anti-GFP Ab. X denotes mutants not discussed in the paper.

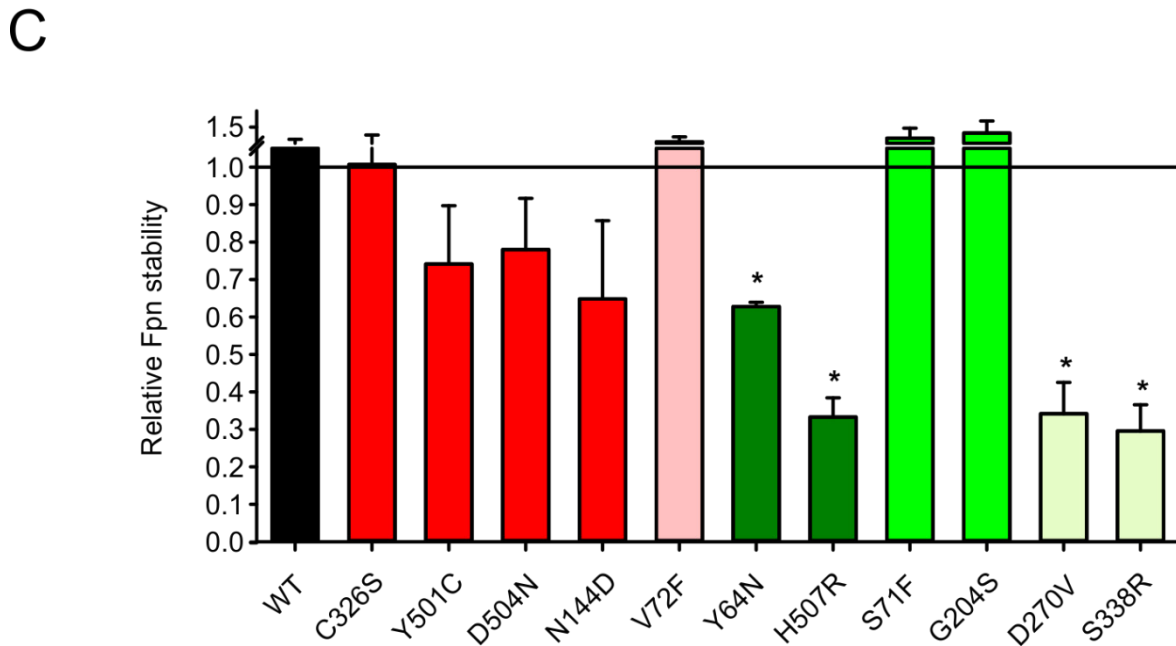
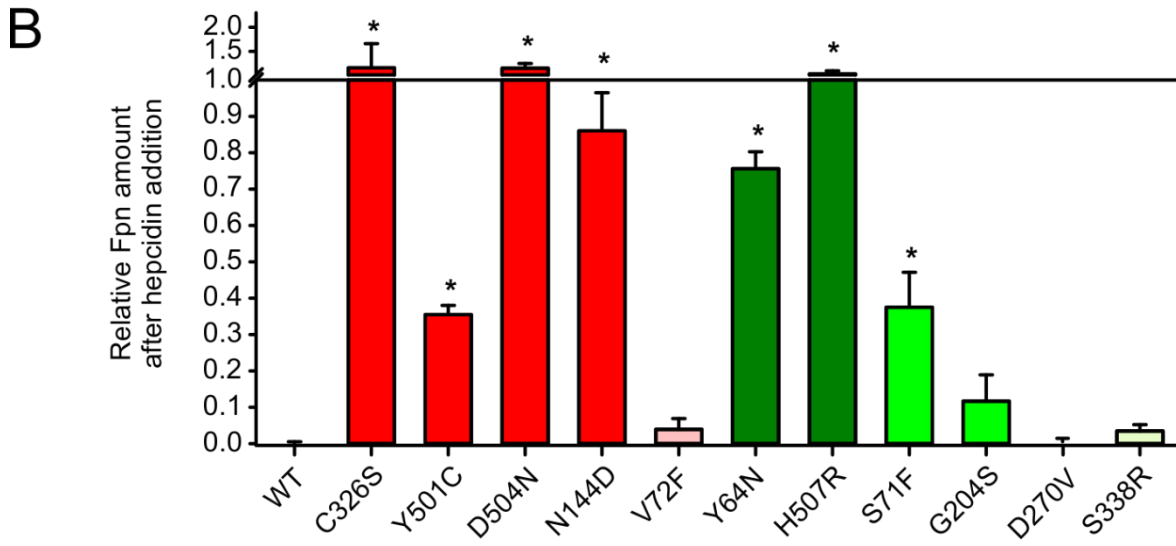
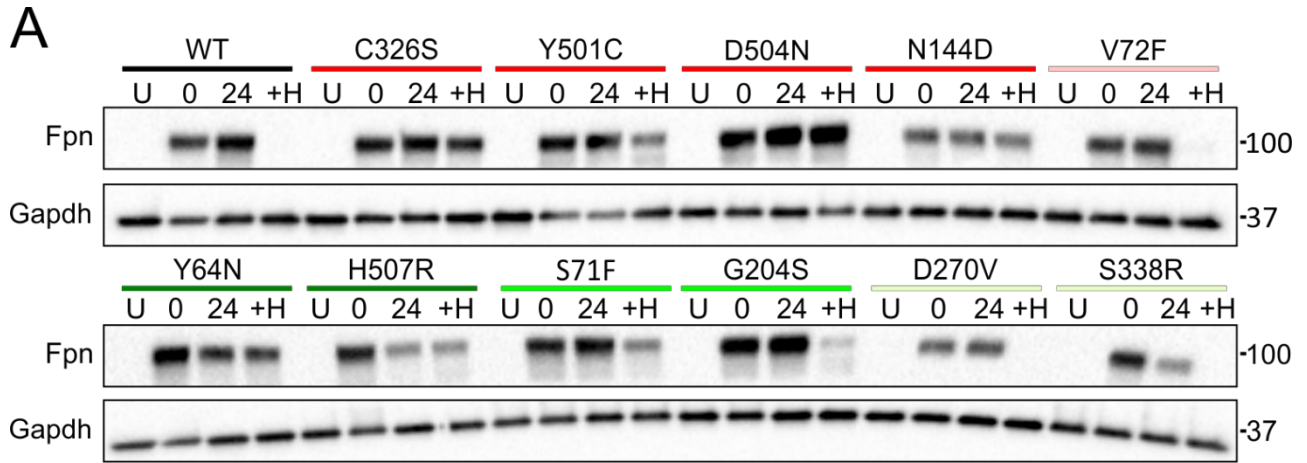


Figure S3: Stability and hepcidin-induced degradation of WT and mutant Fpn. Cells were induced overnight to express hFpn-GFP. The inducer was removed, the cells were washed, and some wells were harvested for the 0 h time point or incubated for another 24 hours \pm 1 μ g/ml hepcidin (0.4 μ M). A) Representative Western blot of WT and mutant hFpn-GFP. Fpn was detected using anti-GFP Ab and GAPDH was used for normalization. U= uninduced Fpn cells, 0= 0 h time-point, 24= 24 h time-point without hepcidin treatment, and H= hepcidin treatment for 24 h. B) Quantification of Fpn degradation by hepcidin. Densitometry was performed on triplicate Western blots from A. GAPDH was used for normalization of the GFP signal. Values of hepcidin-treated samples were further normalized to their respective untreated 24 h control to express results as relative Fpn amount after hepcidin treatment. The two-tailed t-test comparing mutants to WT was employed and the FDR procedure was used to determine significance where * = significant. C) Quantification of Fpn stability. Densitometry was performed on triplicate Western blots from A, and GAPDH was used for normalization of GFP signal. Fpn values at 24 h (non-hepcidin treated) were expressed as a fraction of their respective controls at 0 h. 1= amount of Fpn at the 0 h time point for each respective mutant. Statistical analysis employed the two-tailed one-sample t-test using 1 as the comparison and the FDR procedure was used to determine significance where * = significant. Data shown are means \pm SEM of 3-5 independent experiments.

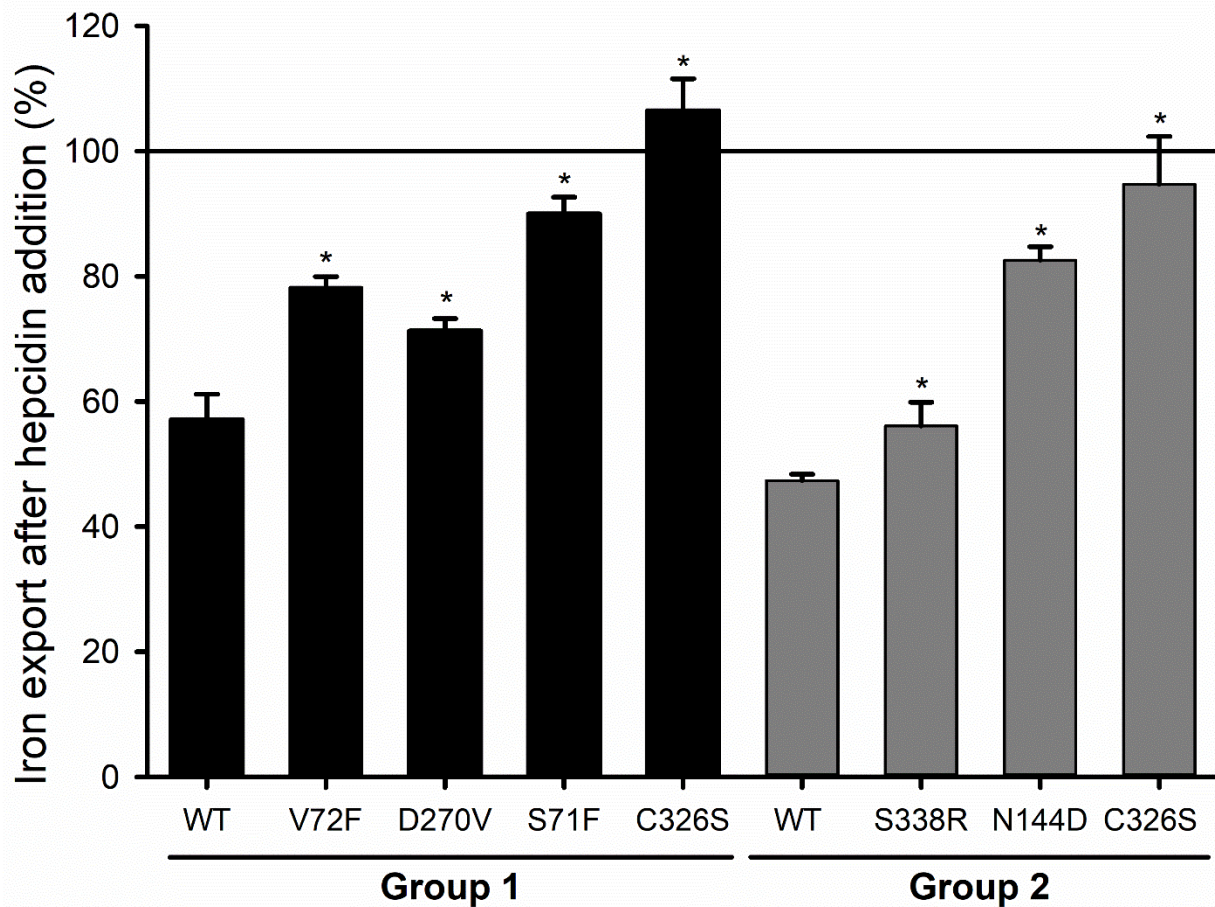


Figure S4: Iron export after hepcidin addition. Cells were loaded with 2mM ^{55}Fe for 48 hours, washed, re-plated, and either left uninduced or were induced by adding doxycycline overnight. Cells were washed again and medium was sampled at multiple time points to measure iron export up to 10 hours \pm hepcidin (Group 1: 0.1 $\mu\text{g}/\text{ml}$, Group 2: 3 $\mu\text{g}/\text{ml}$). The "uninduced" measurement at each time point was subtracted as background. The slope for each "induced" and "induced + hepcidin" sample was determined, and % export after hepcidin treatment calculated. Data shown are means \pm SEM of at least 4 biological replicates. Statistical analysis employed the two-tailed t-test if normally distributed and the two-tailed t-test on ranks if not, comparing each mutant to the WT Fpn analyzed within the same experiment. Once the P-values were determined, the FDR procedure was used to determine significance, which is indicated with *. C326S, a highly hepcidin-resistant mutant, was used in each experiment as a control for assay integrity.

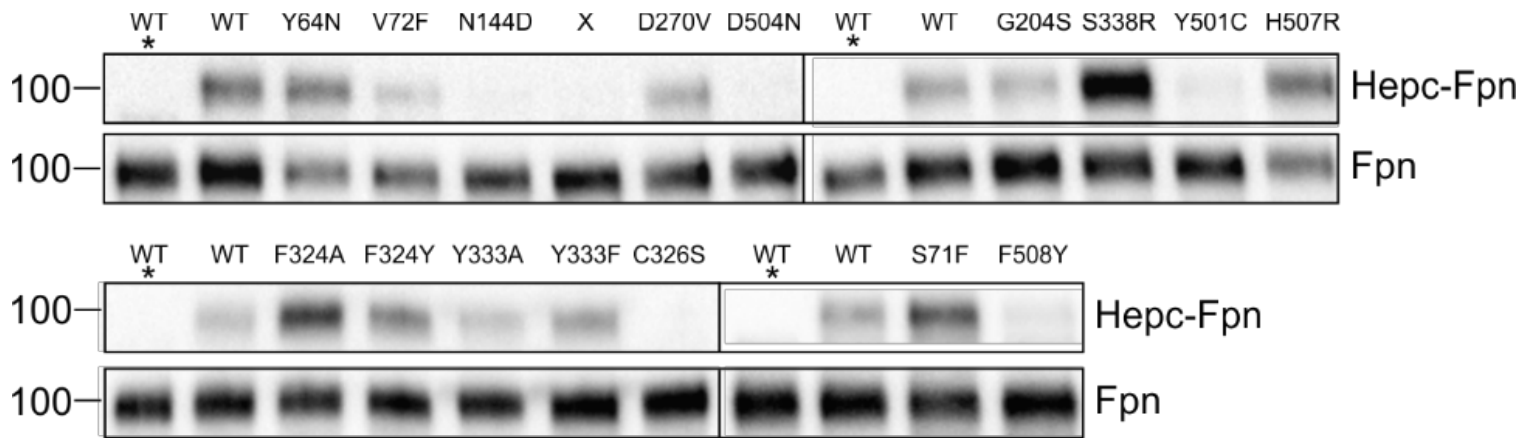


Figure S5: Representative Western blots: hepcidin binding to hFpn. Cells induced to express WT or mutant hFpn-GFP were treated with N-terminally biotinylated hepcidin for 30 minutes, immunoprecipitated with anti-GFP Ab, run under non-reducing conditions, and immunoblotted with streptavidin-HRP or anti-GFP Ab. Hepc-Fpn= hepcidin complexed with Fpn.*= WT with no hepcidin added. X denotes a mutant not discussed in the paper.

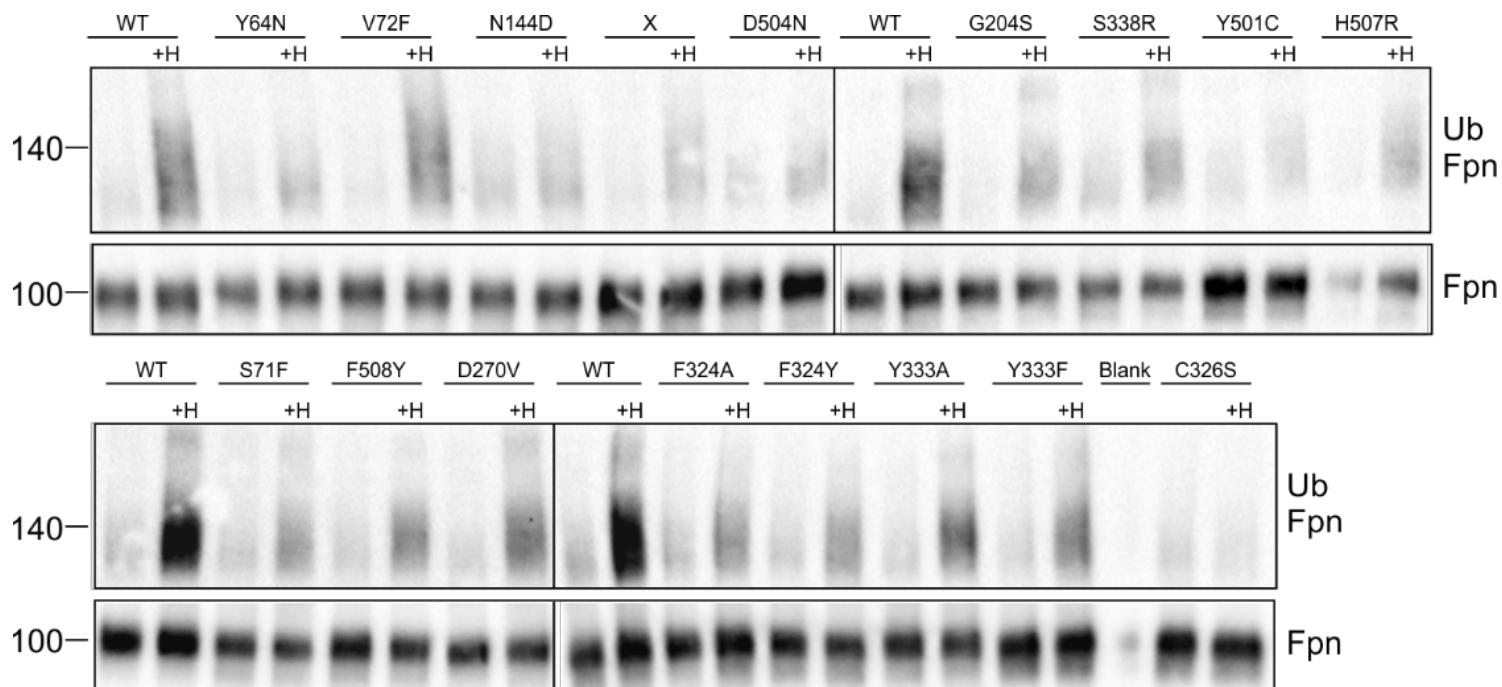


Figure S6: Representative Western blots: ubiquitination of hFpn. Cells expressing WT and mutant hFpn-GFP were treated with hepcidin for 30 minutes, immunoprecipitated with anti-GFP Ab, and immunoblotted with anti-poly/mono ubiquitin Ab (FK2) or anti-GFP Ab. X denotes a mutant not discussed in the paper.

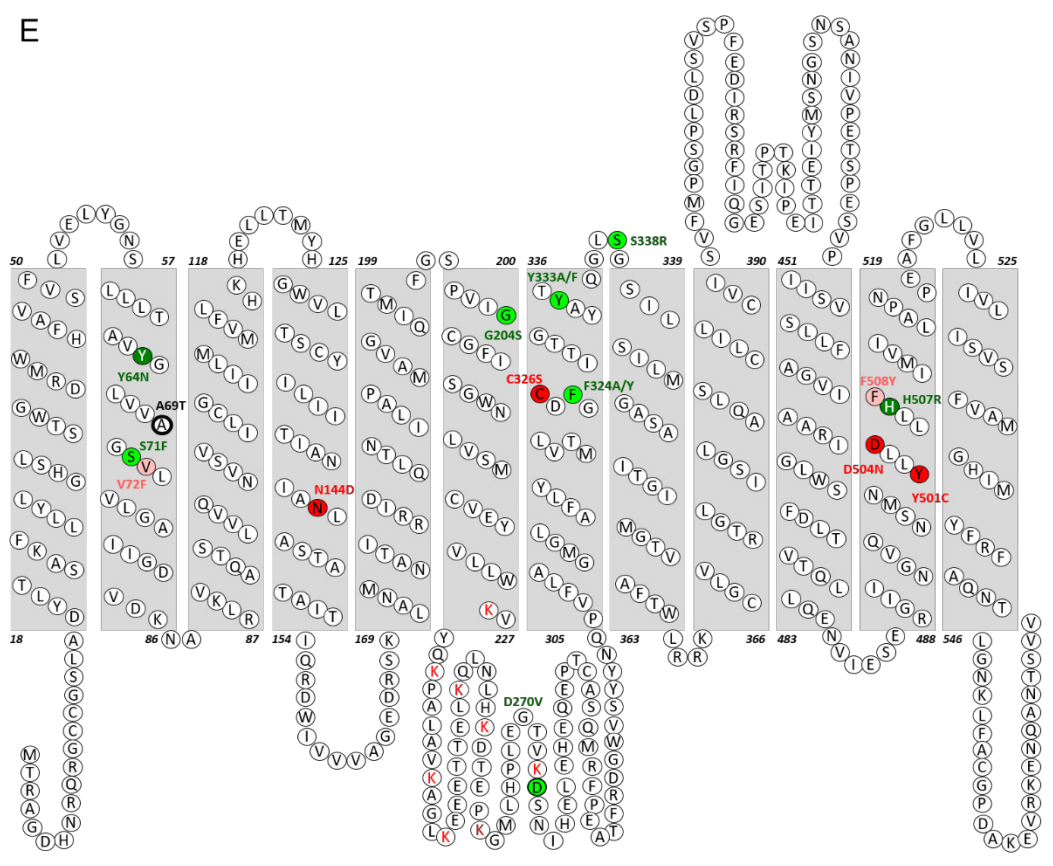
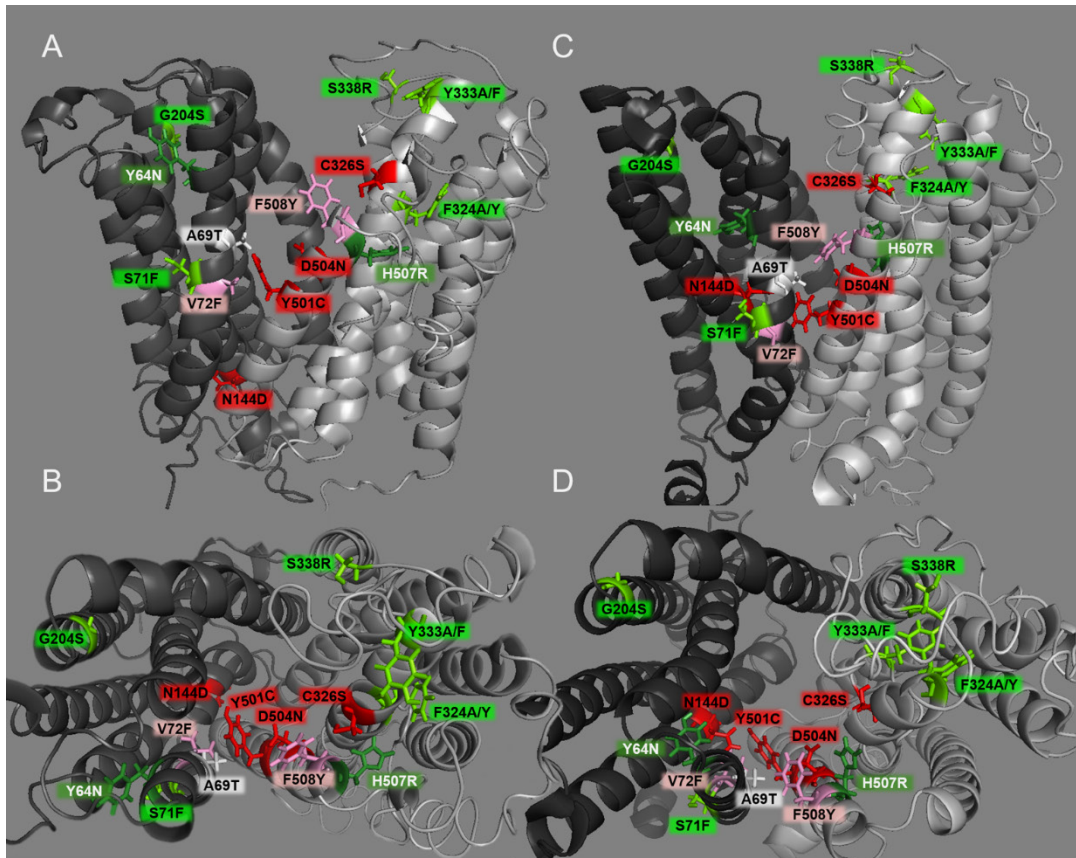


Figure S7: hFpn I-TASSER modeling without or with BdFPN among templates. A,B) Model generated without the Bd2109 crystal structure; side-view and top-view of hFpn in its outward-facing state are shown. C,D) Model generated by including the Bd2109 crystal structure among templates; side-view and top-down view of hFpn in its outward-facing state are shown. D270V is not modeled because it is in the disordered intracellular loop of Fpn. Red/pink color denotes mutants with impaired hepcidin binding, and the green color denotes mutants with intact hepcidin binding but variably impaired ubiquitination. A69T, the white colored mutant, is a recently discovered clinical mutation causing non-classical ferroportin disease that was not experimentally examined in our study. E) 2D Fpn model of A and B. Red Ks (lysines) indicate the residues mutated in the K8R Fpn mutant. For A-E, the bold color denotes severe mutants and lighter color denotes mild and borderline mutants.

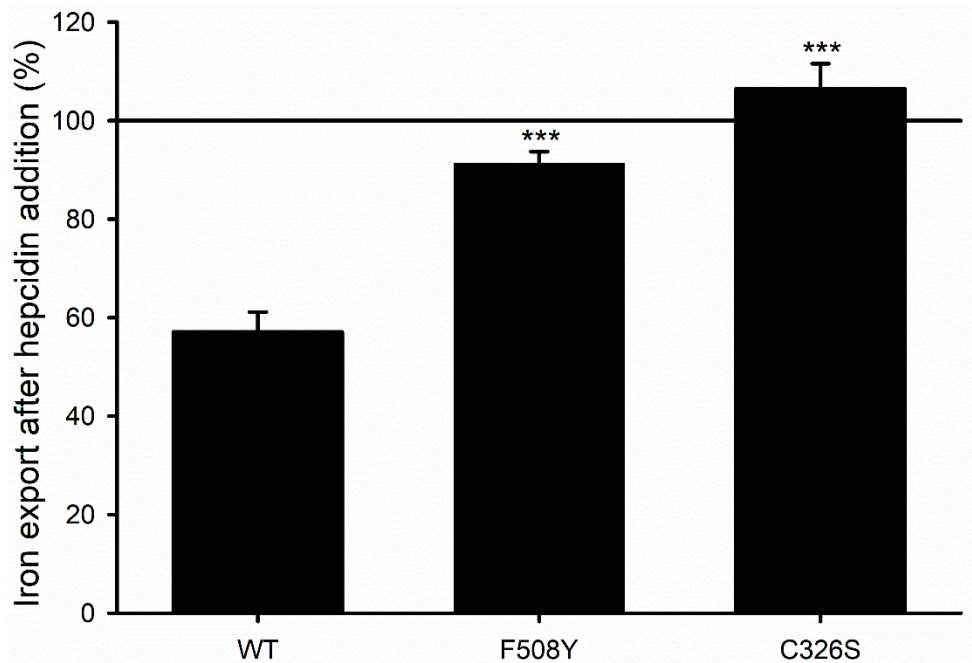


Figure S8: F508Y Fpn mutant is functionally resistant to hepcidin as determined by radiolabeled iron export. Cells were loaded with 2mM ^{55}Fe for 48 hours, washed, replated, and either left uninduced or were induced by adding doxycycline overnight. Cells were washed again, and medium sampled at multiple time points to measure iron export up to 10 hours \pm 0.1 $\mu\text{g/ml}$ hepcidin. The "uninduced" measurement at each time point was subtracted as background. The slope for each "induced" and "induced + hepcidin" sample was determined, and % export after hepcidin treatment calculated. Statistical analysis employed the two tailed t-test comparing each mutant to the WT. Data shown are means \pm SEM of at least 4 biological replicates. *** $P < 0.0005$, ** $P < 0.005$, * $P < 0.05$ by t-test or t-test on ranks if not normally distributed. C326S, a highly hepcidin-resistant mutant, was used in each experiment as a control for assay integrity.

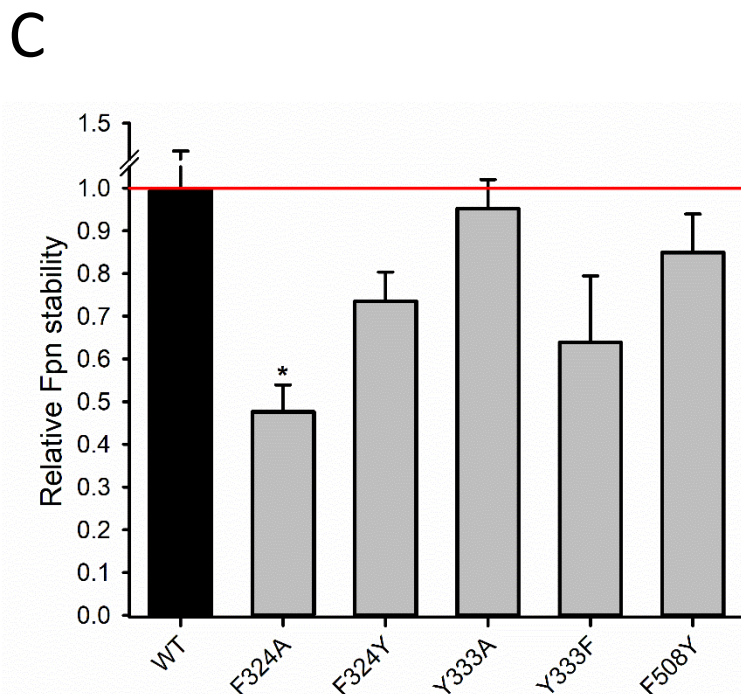
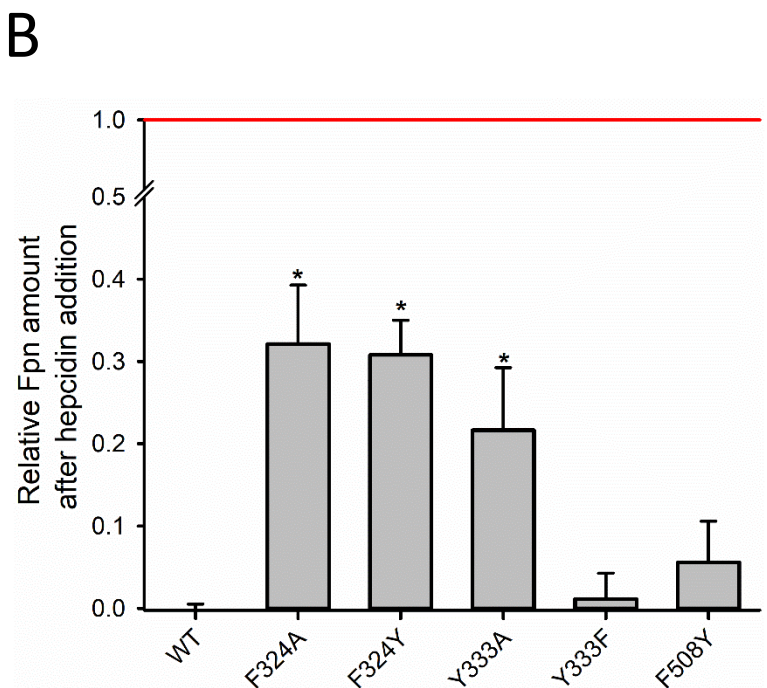
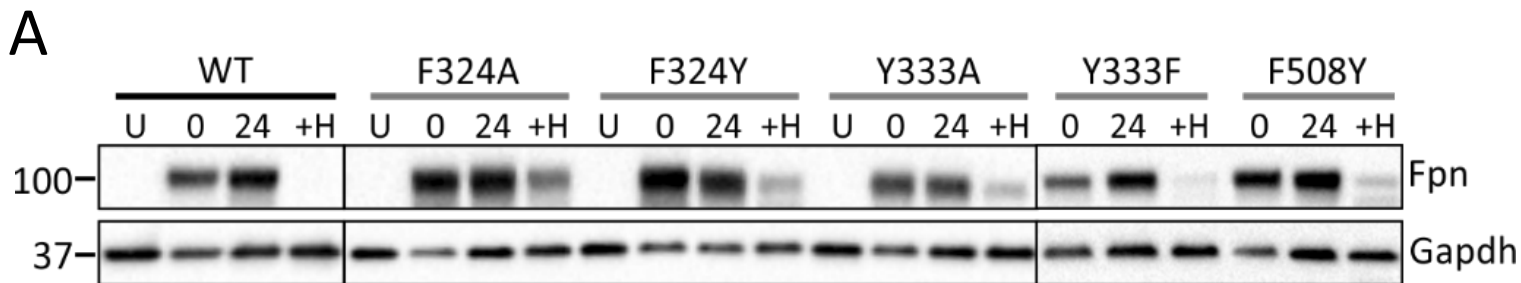


Figure S9: Stability and hepcidin-induced degradation of hFpn. Cells expressing inducible nonclinical Fpn mutants were analyzed with the same approaches as described in Figure S3. Cells were induced overnight to express WT and mutant hFpn-GFP. Doxycycline was removed and cells harvested for the 0 h time point or incubated for another 24 hours \pm 1 μ g/ml hepcidin (0.4 μ M) hepcidin. A) Representative Western blots. B) Quantification of Fpn degradation by hepcidin. C) Quantification of Fpn stability. Densitometry in B and C was performed on triplicate Western blots from A, and an average of two housekeeping proteins was used for normalization (GAPDH and actin). Statistical analysis employed the two-tailed t-test comparing the mutants to WT (B) or the two-tailed one-sample t-test using 1 as the comparison (C) Data shown are means \pm SEM of 3 independent experiments. The FDR procedure was used to determine significance (* = significant).

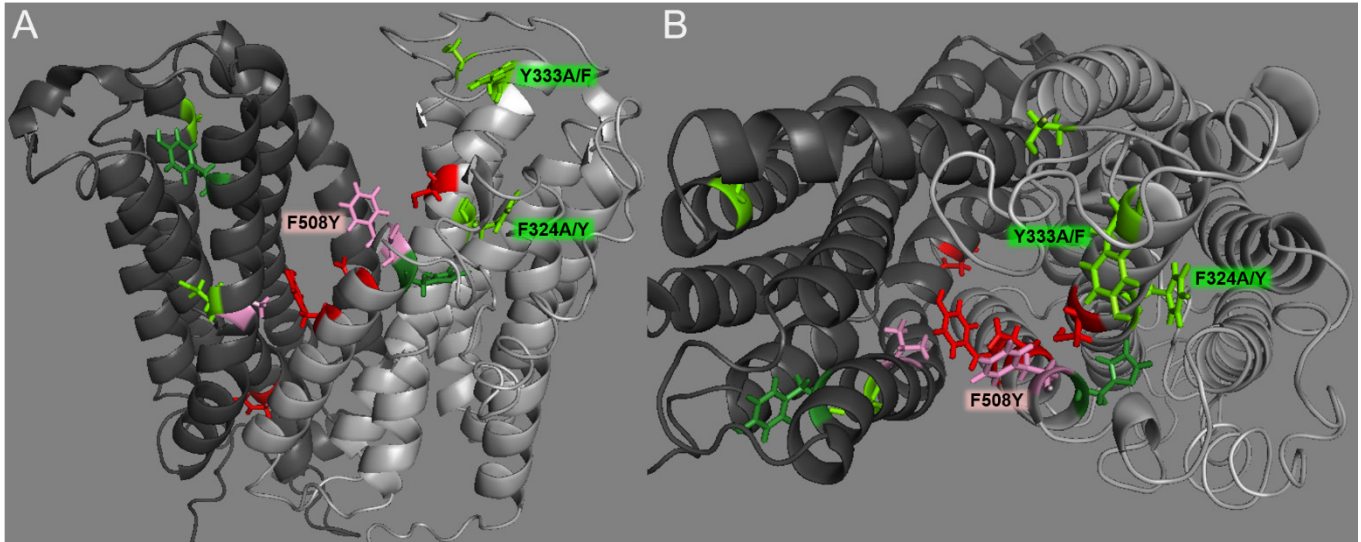


Figure S10: hFpn structure depicting nonclinical mutant residues. A) A side-view of hFpn in its outward-facing state, with the N-terminus on the left and C-terminus on the right. B) Top-down view of hFpn in its outward-facing state. All nonclinical mutants are mild mutants.

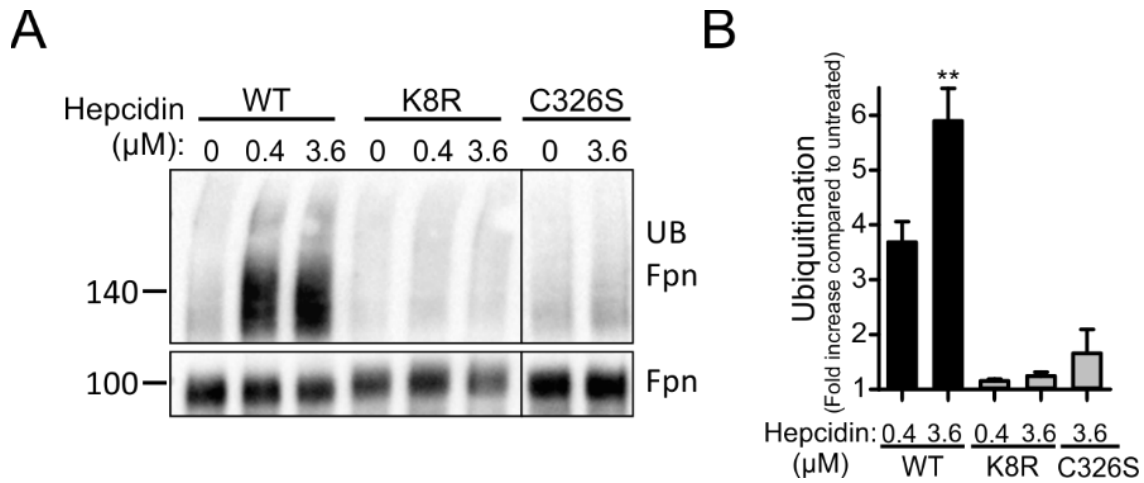
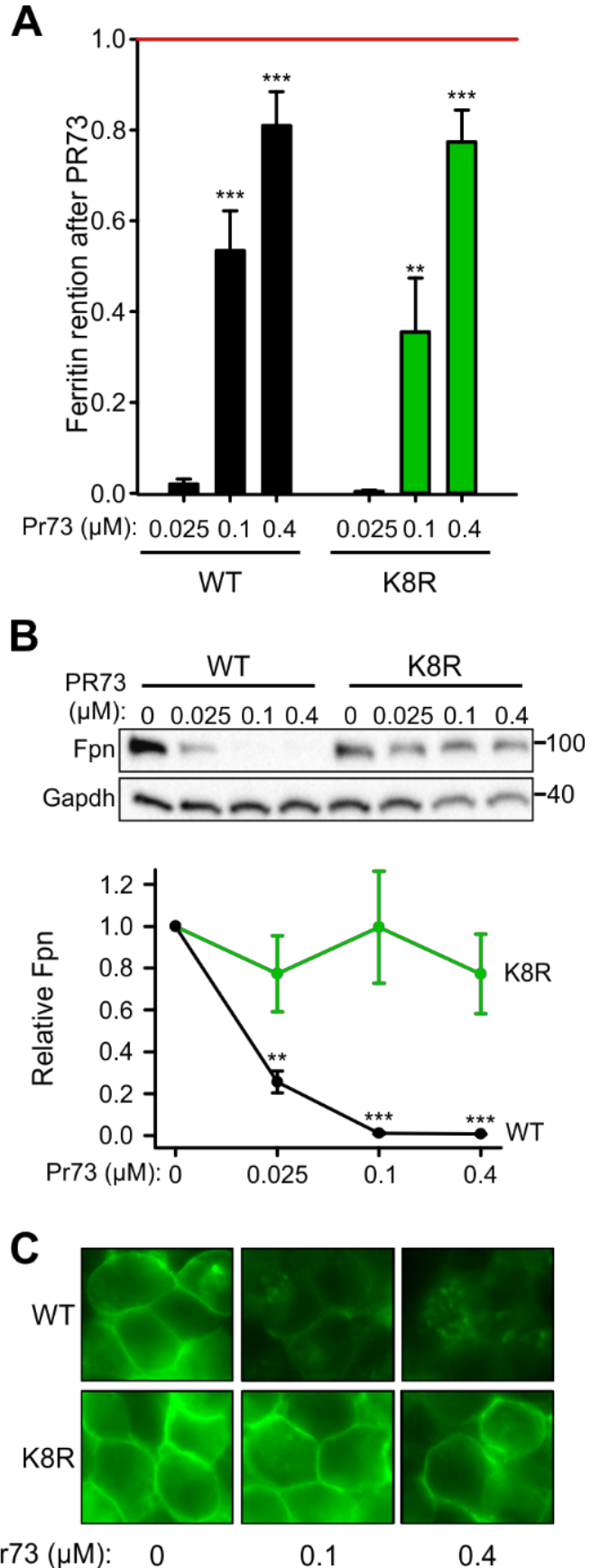


Figure S11: High concentrations of hepcidin do not cause ubiquitination of K8R Fpn. A) hFpn-GFP WT and mutants were treated with hepcidin for 30 minutes, immunoprecipitated with anti-GFP Ab, and immunoblotted with anti-poly/mono ubiquitin Ab (FK2) or anti-GFP Ab. The C326S mutant, which does not bind hepcidin, was used as a control. B) Quantification of triplicate Western blots from A. Ubiquitination was normalized to total Fpn in each sample and then expressed as fold increase over hepcidin-untreated sample. 1= the amount of basal ubiquitination for each respective untreated mutant in the absence of hepcidin. Results are shown as the mean \pm SEM of 3-5 independent experiments. Statistical significance for mutants was achieved only for the WT treated with 3.6 μM hepcidin when employing the two-tailed one-sample t-test using 1 as a comparison.

Figure S12: Evidence for Fpn occlusion by minihepcidin. Cells expressing inducible non-ubiquitinated K8R mutant were compared to those expressing WT Fpn. A) Ferritin retention after hepcidin addition was determined as in Figure 3A. Statistical analysis employed the two-tailed t-test using the respective untreated control for comparison ($***P<0.001$, $**P<0.01$, $*P<0.05$). Data shown are the mean \pm SEM of 3 independent experiments. B) Lysates from A were analyzed by Western blotting. Top: representative Western blot. Bottom: densitometry of triplicate Western blots. Fpn signal was first normalized to GAPDH, then expressed as the fraction of respective untreated control (no hepcidin treatment). Data shown are the mean \pm SEM of 3 independent experiments. For A and B, statistical analysis employed the two-tailed one-sample t-test using 1 as the comparison ($***P<0.001$, $**P<0.01$, $*P<0.05$). C) Microscopy of samples in A after 24 hours.



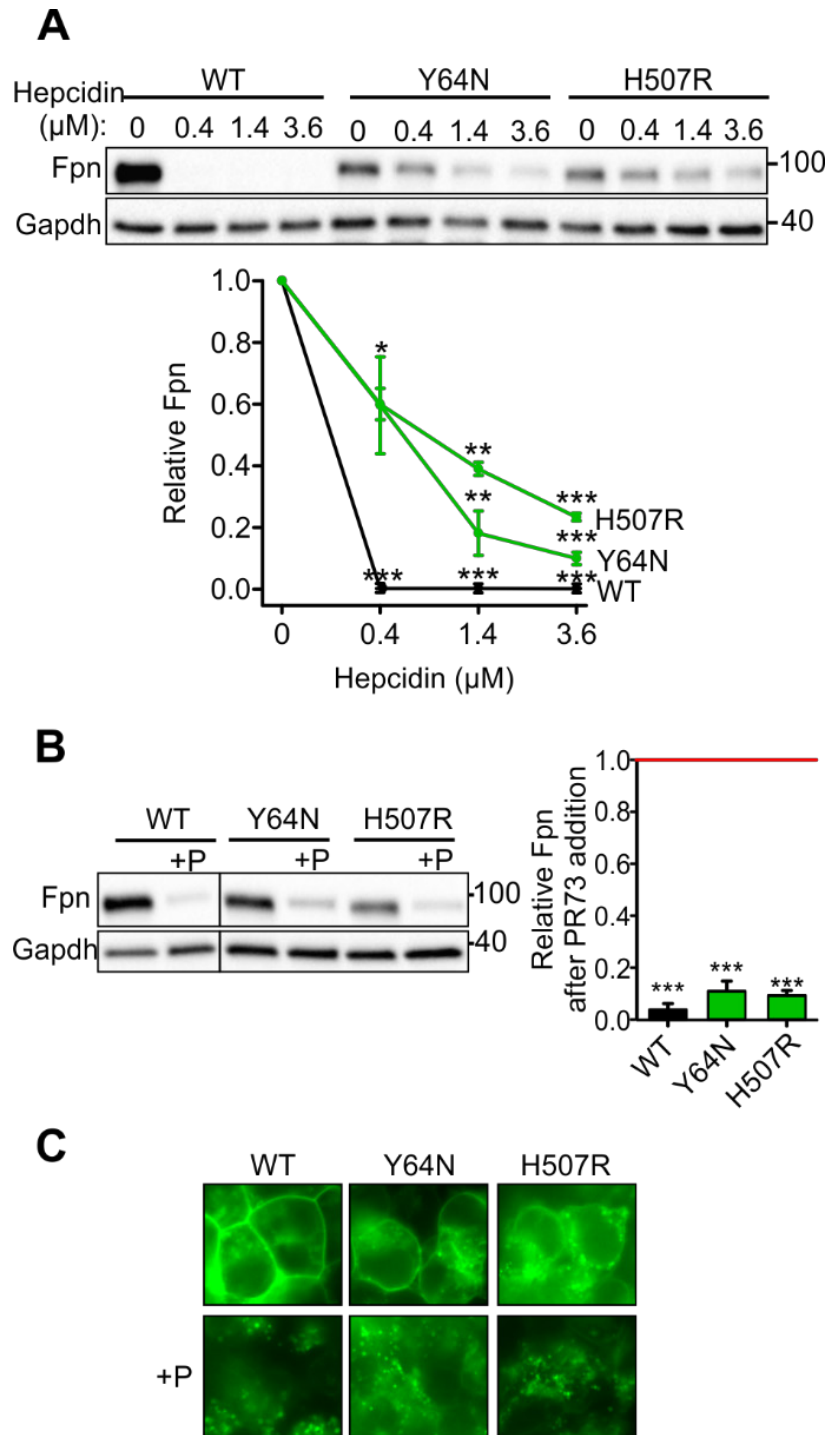


Figure S13: H507R and Y64N Fpn are degraded in the presence of high hepcidin or minihepcidin concentrations. A) Cells expressing inducible Y64N or H507R mutations were compared to those expressing WT Fpn in the presence of 0-3.6 μM hepcidin. Lysates were analyzed by Western blotting. Top: representative Western blot. Bottom: densitometry of triplicate Western blots. Fpn signal was first normalized to GAPDH, then

expressed as the fraction of respective untreated control (no hepcidin treatment). B) Cells expressing inducible Y64N or H507R mutations were compared to those expressing WT Fpn in the presence or absence of 3.6 μ M PR73. Lysates were analyzed by Western blotting 24 hours after treatment. Left: representative Western blot. Right: densitometry of triplicate Western blots. Fpn signal was first normalized to GAPDH and then expressed as the fraction of respective untreated control (no PR73 treatment). Data shown are the mean \pm SEM of 3 independent experiments. For A and B statistical analysis employed the two-tailed one-sample t-test using 1 as the comparison (**P<0.001, **P<0.01, *P<0.05). C) Microscopy of WT and mutant cells 24 hours \pm PR73 treatment.

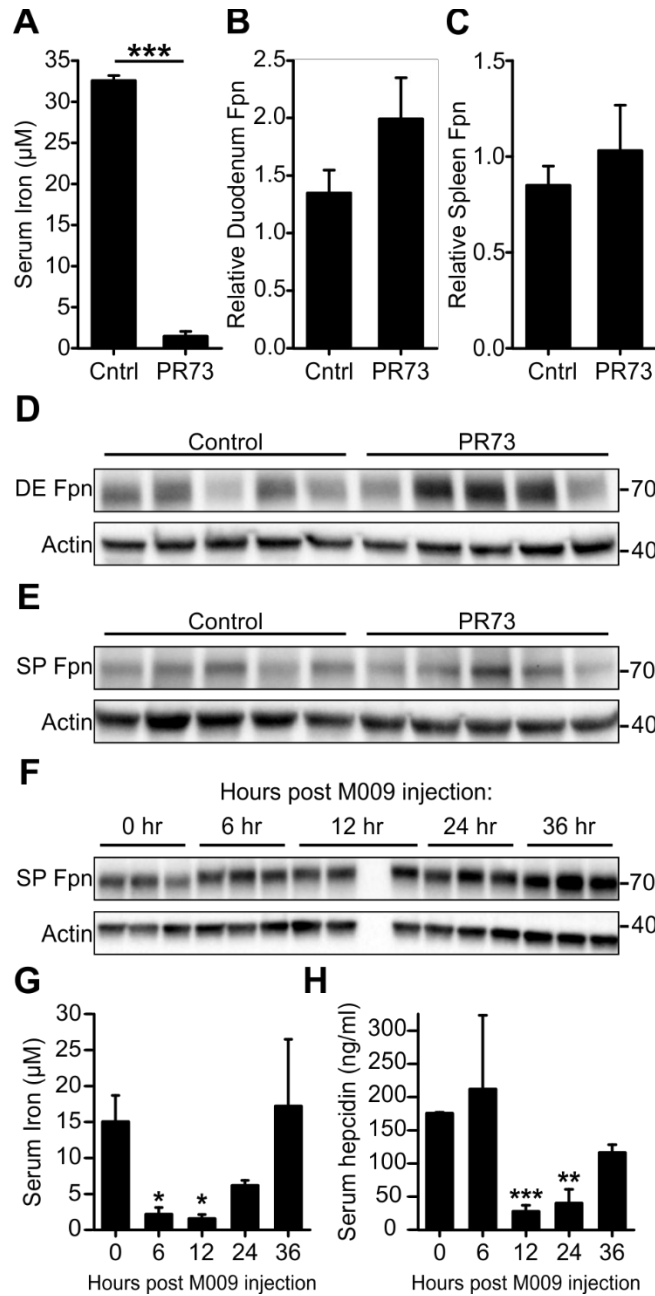


Figure S14: *In vivo* Fpn levels do not change after minihepcidin administration despite drastic decrease in serum iron. (A-E) WT mice were injected two times with 60 nmoles of PR73 and analyzed 4 hours after the second injection. A) Serum iron. B) Quantitation of duodenal Fpn levels (corresponding to the Western blot in D, normalized to actin). C) Quantitation of splenic Fpn levels (corresponding to the Western blot in E, normalized to actin). A-C) Cntrl= control. D) Western blot of Fpn and actin in duodenal enterocytes. E) Western blot of Fpn and actin in spleen. (F-H) th3 mice received a single injection of M009 minihepcidin, and tissues were harvested after 0, 6, 12, 24 and 36 h. F) Western blot of Fpn in the spleen. G) Serum iron. H) Serum hepcidin. Graphs show the

mean \pm SEM. For A, B, C, G and H, statistical analysis employed the two-tailed t-test using either the control (A-C) or the zero hour time point (G,H) for comparison (**P<0.001, **P<0.01, *P<0.05).

SUPPLEMENTAL REFERENCES

S1. Lok CY, Merryweather-Clarke AT, Viprakasit V, Chinthammitr Y, Srichairatanakool S, Limwongse C, Oleesky D, et al. Iron overload in the Asian community. *Blood* 2009;114:20-25.

S2. Sham RL, Phatak PD, West C, Lee P, Andrews C, Beutler E. Autosomal dominant hereditary hemochromatosis associated with a novel ferroportin mutation and unique clinical features. *Blood Cells, Molecules, and Diseases* 2005;34:157-161.

S3. Letocart E, Le GG, Majore S, Ka C, Radio FC, Gourlaouen I, De BC, et al. A novel missense mutation in SLC40A1 results in resistance to hepcidin and confirms the existence of two ferroportin-associated iron overload diseases. *Br.J Haematol.* 2009;147:379-385.

S4. Callebaut I, Joubrel R, Pissard S, Kannengiesser C, Gérolami V, Ged C, Cadet E, et al. Comprehensive functional annotation of 18 missense mutations found in suspected hemochromatosis type 4 patients. *Human Molecular Genetics* 2014;23:4479-4490.

S5. Wallace DF, Clark RM, Harley HA, Subramaniam VN. Autosomal dominant iron overload due to a novel mutation of ferroportin1 associated with parenchymal iron loading and cirrhosis. *J Hepatol* 2004;40:710-713.

S6. Pelucchi S, Mariani R, Salvioni A, Bonfadini S, Riva A, Bertola F, Trombini P, et al. Novel mutations of the ferroportin gene (SLC40A1): analysis of 56 consecutive patients with unexplained iron overload. *Clin Genet* 2008;73:171-178.

S7. Rivard SR, Lanzara C, Grimard D, Carella M, Simard H, Ficarella R, Simard R, et al. Autosomal dominant reticuloendothelial iron overload (HFE type 4) due to a new missense mutation in the FERROPORTIN 1 gene (SLC11A3) in a large French-Canadian family. *Haematologica* 2003;88:824-826.

S8. Mayr R, Griffiths WJ, Hermann M, McFarlane I, Halsall DJ, Finkenstedt A, Douds A, et al. Identification of mutations in SLC40A1 that affect ferroportin function and phenotype of human ferroportin iron overload. *Gastroenterology* 2011;140:2056-2063, 2063.

S9. Yamakawa N, Oe K, Yukawa N, Murakami K, Nakashima R, Imura Y, Yoshifuji H, et al. A Novel Phenotype of a Hereditary Hemochromatosis Type 4 with Ferroportin-1 Mutation, Presenting with Juvenile Cataracts. *Intern Med* 2016;55:2697-2701.

S10. Le Lan C, Mosser A, Ropert M, Detivaud L, Loustaud-Ratti V, Vital-Durand D, Roget L, et al. Sex and acquired cofactors determine phenotypes of ferroportin disease. *Gastroenterology* 2011;140:1199-1207 e1191-1192.

- S11. Santos PC, Cancado RD, Pereira AC, Schettert IT, Soares RA, Pagliusi RA, Hirata RD, et al. Hereditary hemochromatosis: mutations in genes involved in iron homeostasis in Brazilian patients. *Blood Cells Mol Dis* 2011;46:302-307.
- S12. Zaahl MG, Merryweather-Clarke AT, Kotze MJ, van der Merwe S, Warnich L, Robson KJ. Analysis of genes implicated in iron regulation in individuals presenting with primary iron overload. *Hum Genet* 2004;115:409-417.
- S13. Lee PL, Gaasterland T, Barton JC. Mild iron overload in an African American man with SLC40A1 D270V. *Acta Haematol* 2012;128:28-32.
- S14. Wallace DF, Dixon JL, Ramm GA, Anderson GJ, Powell LW, Subramaniam VN. A novel mutation in ferroportin implicated in iron overload. *J.Hepatol.* 2007;46:921-926.
- S15. Arezes J, Jung G, Gabayan V, Valore E, Ruchala P, Gulig PA, Ganz T, Nemeth E, Bulut Y. Hepcidin-induced hypoferremia is a critical host defense mechanism against the siderophilic bacterium *Vibrio vulnificus*. *Cell Host Microbe*. 2015 Jan 14;17(1):47-57. doi: 10.1016/j.chom.2014.12.001.
- S16. Qiao B, Sugianto P, Fung E, et al. Hepcidin-induced endocytosis of ferroportin is dependent on ferroportin ubiquitination. *Cell Metab*. 2012;15(6):918-924.
- S17. Mitchell CJ, Shawki A, Ganz T, Nemeth E, Mackenzie B. Functional properties of human ferroportin, a cellular iron exporter reactive also with cobalt and zinc. *Am J Physiol Cell Physiol*. 2014;306(5):C450-459.
- S18 Stefanova D, Raychev A, Arezes J, Ruchala P, Gabayan V, Skurnik M, Dillon BJ, Horwitz MA, Ganz T, Bulut Y, Nemeth E. Endogenous hepcidin and its agonists mediate resistance to selected infections by clearing non-transferrin-bound iron. *Blood*. 2017 Jul 20;130(3):245-257. doi: 10.1182/blood-2017-03-772715.
- S19. Casu C, Oikonomidou PR, Chen H, Nandi V, Ginzburg Y, Prasad P, Fleming RE, Shah YM, Valore EV, Nemeth E, Ganz T, MacDonald B, Rivella S. Minihepcidin peptides as disease modifiers in mice affected by β -thalassemia and polycythemia vera. *Blood*. 2016 Jul 14;128(2):265-76. doi: 10.1182/blood-2015-10-676742.
- S20. Kautz L, Gabayan V, Wang X, et al. Testing the iron hypothesis in a mouse model of atherosclerosis. *Cell Rep*. 2013;5(5):1436-1442.
- S21. Aschemeyer S, Gabayan V, Ganz T, Nemeth E, Kautz L. Erythroferrone and matriptase-2 independently regulate hepcidin expression. *Am J Hematol*. 2017;92(5):E61-E63.